SPECTRAL RECONSTRUCTION METHOD
FOR LIQUID VELOCITY MEASUREMENT
BEYOND THE NYQUIST LIMIT

Stéphane FISCHER*, Philippe SCHMITT**, Benoît SCHWALLER***

IMFS, UMR 7507 ULP-CNRS
IUT Louis Pasteur
allée d'Athènes
67300 SCHILTIGHEIM
* stephane.fischer@convergence.u-strasbg.fr,
** schmitt@convergence.u-strasbg.fr,
*** brs@convergence.u-strasbg.fr

ABSTRACT

In pulsed Doppler velocimetry, one of the main constraints is the opposite relation binding the exploration depth and the maximum measurable velocity (Nyquist velocity). Thus for a value higher than the Nyquist limit, the Doppler spectrum is aliased (Shannon Theorem) and the estimated velocity is false. In some applications, this limit is penalizing. Especially, the ultrasonic velocity profiles measurement in sewerage is compromised.

A method allowing velocity measurements beyond the Nyquist limit is proposed. It is based on a technique from weather radars using multiple pulse repetition frequency (PRF). Each folding up, which is different for each PRF, adds information in order to resolve the velocity ambiguity. The proposed algorithm recombines the aliased spectra obtained for each PRF in order to reproduce the original Doppler spectrum. Velocity can thus be calculated on a spectrum not splited by folding up.

With this new method, the limit is not given any more for the maximum frequency in the Doppler spectrum but for the maximum width of this spectrum. Indeed, the only constraint is that the periodisation of the spectrum, which is related to the sampling, does not cause any overlapping of the copies of the original spectrum.

Keywords: range-velocity ambiguity, pulsed ultrasonic Doppler velocimetry, multiple pulse repetition frequency, power spectrum density (PSD)

INTRODUCTION

With the use of ultrasonic Doppler Method for velocity measurements, the pulse repetition frequency (PRF) gives both the exploration depth and the sample rate of the Doppler wave. This results in a bond between the maximum detectable velocity and the exploration depth, also known as range-velocity ambiguity.

The maximum velocity, noted Nyquist velocity v_{Ny}, is given, for the situation given figure 1, by equation:

$$v_{Ny} = \frac{c^2 \tan \beta}{8 f_0 h} \tag{1}$$

with:

h : water height
β : angle between flow and transducer axis
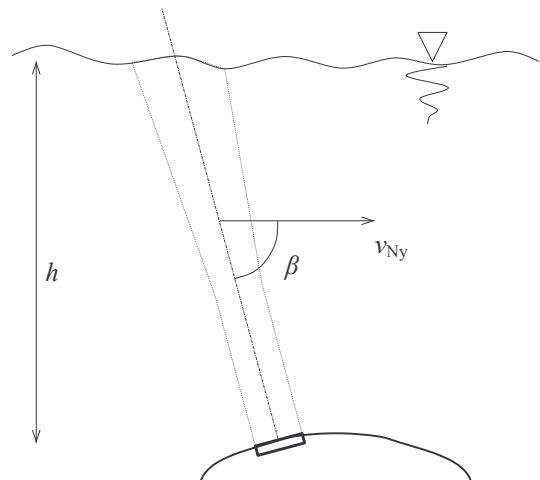c : acoustic velocity
f_0 : ultrasound frequency.

Fig. 1 Principle of flow scan. The transducer sends an ultrasonic burst into the pipe (height h) with an angle β compared to the flow direction (represented by velocity vector v_{Ny}).

The fixed goal is the development of a fluxmeter able to deliver velocity information up to 3 m/s in a 1m depth pipe. These limits include a majority of situations for most pipes present in sewer networks.

In these hydraulic flows, the particles with a higher radius than 750μm move by saltation, and thus be inappropriate ultrasound tracers.

Moreover, reflection on a particle target implies that ultrasound wavelengths are small compared to the particle size [2]. Thus, an emission frequency of 1MHz is an adequate solution. According to equation (1), and with a angle of β= 75°, the Nyquist limit is about 1 m/s, value three times smaller than the desired value.

In order to solve the range-velocity ambiguity, the use of different repetition frequencies has been proposed in the Doppler weather radar domain [3, 4].

This technique, also named *staggered PRT*, *MPDA* (*Multi PRF Dealiasing Algorithm*) or *Dual PRF* is used in addition to *pulse-pair* algorithms. It is based on the calculation of the mean velocity for every PRF, than combine these velocities in order to retrieve the true velocity in the considered spatial volume.

Spectrum mean frequency estimated by the *pulse-pair* method is given, for one given PRF, in the [-PRF/4; PRF/4] interval. Thus, a disadvantage of this method is the biasing of the velocity estimation to a value of PRF/2 for frequencies near on the values $\left(k+\dfrac{1}{2}\right)\dfrac{PRF}{2}$ (k integer). The probability to observe this bias increases for large spectrums and small signal to noise ratios.

This paper focuses on velocity estimation by spectral analysis. The true Doppler spectrum is extrapolated from a batch of folded up spectrums obtained by undersampling the Doppler signal at different PRF. First results obtained with simulation are discussed.

PRINCIPLE

Signal characteristics

The Doppler signal resulting from the echo demodulation in phase and quadrature from particles present in the fluid is noted s(t). It is a complex signal with random phase, available only in its sampled form s*(t) at the sampling frequency:

$$f_e = \frac{1}{T_e} = \frac{\omega_e}{2\pi} \qquad (2)$$

$G(\omega)$ is the power spectral density (PSD) of the continuous signal s(t). The PSD of the sampled signal (Figure 2) can be written as:

$$G*(\omega) = \frac{1}{T_e^2} \sum_{k=-\infty}^{+\infty} G(\omega - k\omega_e) \qquad (3)$$

This density has a limited bandwidth $\Delta\omega$, centered on the Doppler pulsation ω_{Dmed}, proportional to the fluid velocity according to the Doppler effect [9]:

$$G(\omega) = 0 \qquad \forall \omega \notin \left]\omega_{Dmed} - \frac{\Delta\omega}{2}; \omega_{Dmed} + \frac{\Delta\omega}{2}\right[\qquad (4)$$

Moreover, the velocity of the fluid is considered to be contained in a specific range, corresponding to a spectral band of $2\omega_M$. We consider:

$$G(\omega) = 0 \qquad \forall \omega \notin \left]-\omega_M; \omega_M\right[\qquad (5)$$

General description of the method

Within the traditional framework of the Shannon theorem, the sampling frequency is choose such as :

$$\omega_e > 2\omega_M \qquad (6)$$

Thus, in figure 2, the middle graph present the PSD of the signal sampled at a frequency f_e respecting this theorem. The PSD of the continuous signal (in the upper graph) can be obtained when considering the interval $\left]-\omega_M; \omega_M\right[$.

On the other hand, when using smaller sampling rates, the signal is undersampled and its spectrum is aliased. When considering the interval $\left]-\omega_M; \omega_M\right[$ (interval $\left]-1;+1\right[$ in the lower graph, figure 2), there is an ambiguity on which spectrum is the truth.
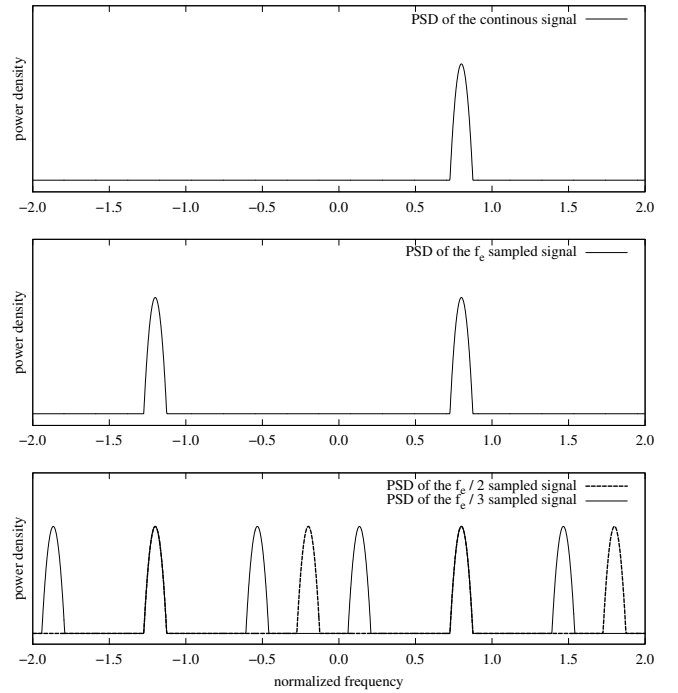

Fig. 2 Effect of folding up according to various sampling rates. The frequency is normalized by f_M, the undersampling factors are 2 and 3.

Undersampling induces a loss of information. Nevertheless, in the case of a signal with limited bandwidth, this loss can be compensated by the use of several spectral densities of the same signal resulting from a sampling at different frequencies. $M(\omega)$ is a combination of the spectral densities of the undersampled signal at various frequencies. An expression of $M(\omega)$ is searched, as well as a criterion on $M(\omega)$ indicating the spectral origin of the energy.

As shown in equation (3), the PSD of the sampled signal can be described as the sum between the spectrum of the continuous signal and infinity of images of this spectrum shifted in frequency (copies). This spectral shift depends only on the sampling frequency. Thus for several different sample frequencies, only the copies will have been moved, whereas

the part of the spectrum corresponding to the continuous signal is always at the same position. When considering the multiplication of the spectra, it is clear that the resulting spectral function has its maximum value where the maxima of the different PSD coincide. This coincidence is systematic at the position of the original spectrum. Elsewhere, the spectrum coincidence will depend on the position(s) of the maximum(s) in the original spectrum and on the sampling rates used.

We consider two sampling rates as well as their associated PSD of the undersampled signal:

$$\begin{cases} f_{e1} = \dfrac{\omega_{e1}}{2\pi}, & G_1^*(\omega) \\ f_{e2} = \dfrac{\omega_{e2}}{2\pi}, & G_2^*(\omega) \end{cases} \tag{7}$$

$M(\omega)$ is the product of these densities:

$$\begin{aligned} M(\omega) &= G_1^*(\omega) \cdot G_2^*(\omega) \\ &= \frac{1}{T_{e1}^2 T_{e2}^2} \sum_{k1=-\infty}^{+\infty} \sum_{k2=-\infty}^{+\infty} G(\omega - k_1\omega_{e1}) \cdot G(\omega - k_2\omega_{e2}) \end{aligned} \tag{8}$$

The conditions on the sampling rates have to be determined so that only the parts corresponding to the original power density in the densities obtained by undersampling have their maxima which coincide. So, the maximum of energy takes place at the noted pulsation $\omega_{D\max}$ defined by:

$$\omega_{D\max} = \underset{\omega}{\arg\max}(M(\omega)) = \underset{\omega}{\arg\max}(G(\omega)) \tag{9}$$

with $\underset{\omega}{\arg\max}$ the function that gives the spectral position of the maximum of power.

By identifying the maximum of the multiplication of the densities from the signal, sampled at various frequencies, and by considering the conditions carried out, one has an indication on the spectral localization of the maximum of energy in the continuous signal.

The subtraction of a portion of energy (represented by a Dirac impulse δ) at this frequency is considered. This implies that the maximum is moved. By recomputing the product and by locating the position of the new maximum, one can locate the presence of energy at another frequency than that of the initial maximum. It is then possible to apply this property in a recursive way in order to rebuild the original power spectral density.

Because this treatment is numerical, the subtraction cannot be applied directly to the spectrum of the continuous signal; on the other hand this one can result in the subtraction of a Dirac comb, defined by $sha_{\omega_e} = \sum_{k=-\infty}^{+\infty} \delta(\omega - k\omega_e)$, to the spectrum of the sampled signal. Thus, the operation of subtraction:

$$G(\omega) - \varepsilon\delta(\omega - \omega_{D\max}) \tag{10}$$

results in:

$$\begin{aligned} &\frac{1}{T_e^2} \sum_{k=-\infty}^{+\infty} G(\omega - k\omega_e) - \varepsilon\delta(\omega - k\omega_e - \omega_{D\max}) \\ =\ & G^*(\omega) - \frac{\varepsilon}{T_e^2} \sum_{k=-\infty}^{+\infty} \delta(\omega - k\omega_e - \omega_{D\max}) \\ =\ & G^*(\omega) - \frac{\varepsilon}{T_e^2} sha_{\omega_e}(\omega - \omega_{D\max}) \end{aligned} \tag{11}$$

The rebuilding of the power spectral density of the continuous signal is carried out by starting with a null density,

then by accumulating at each stage of the recurrence a portion of the energy identified at the frequency of the detected maximum. Conversely, the densities of the undersampled signal are gradually cut down by the algorithm. The iteration is stopped when the remaining energy in these densities is close to zero.

Sampling frequency determination

The depth of exploration is the first constraint on the choice of the sampling rates. This constraint acts through the time of flight of the wave. Thus, whatever the $\omega_{e\{i\}}$, it is necessary to respect:

$$\frac{cT_{e\{i\}}}{2} > \frac{h}{\sin\beta} \tag{12}$$

The condition imposed by the algorithm is deduced from the equations (8) and (9) by introducing the conditions (4) and (5) and by stipulating that the copies should not be superimposed:

$$|k_1\omega_{e1} - k_2\omega_{e2}| > \Delta\omega \tag{13}$$

for all k_1 and k_2 integers such as : $\begin{cases} |k_1\omega_{e1}| < \omega_M \\ |k_2\omega_{e2}| < \omega_M \end{cases}$

An undersampling factor $k_{se\{i\}}$ (real number) is defined for each sampling frequency, such as:

$$2\omega_M = k_{se\{i\}}\omega_{e\{i\}} \tag{14}$$

This factor link the sampling frequency that would be necessary to respect the Shannon theorem ($2\omega_M$) and the effective sampling frequency ($\omega_{e\{i\}}$), respecting the depth constraint described by equation (12).

As the spectrum width $\Delta\omega$ is *a priori* unknown, the distance between the various components (copies) of the folded up spectra have to be maximized. By imposing k_{se1} such as the constraint of depth is respected, $k_{se2} > k_{se1}$ is determined such as (by introducing equation (14) in condition (13)):

$$\underset{k_{se2}}{\arg\max}\left(\underset{k_1,k_2}{\min}\left(\left| \frac{k_1}{k_{se1}} - \frac{k_2}{k_{se2}} \right| \right) \right) \tag{15}$$

for all k_1 and k_2 integers such as : $\begin{cases} |2k_1| < k_{se1} \\ |2k_2| < k_{se2} \end{cases}$

Thus, taking an undersampling factor $k_{se1} = 2$, induces $k_{se2} = 3$ and the limiting spectrum width $\Delta\omega = \dfrac{\omega_M}{3}$.

Spectral density computing

In practice, the spectra are computed with the numerical algorithm of Fast Fourier Transform (FFT). Since algebraic operations have to be carried out between spectra obtained from different sampling frequencies ($f_{e\{i\}}$), it is necessary to choose for each sampling rate the suitable sample numbers $N_{e\{i\}}$ in order to obtain, in each case, the same spectral resolution δf_e . This implies:

$$\delta f_e = \frac{f_{e\{i\}}}{N_{e\{i\}}} \tag{16}$$

The standard algorithm of the Fast Fourier Transform (FFT), initially proposed by Cooley and Tuckey, requires a sample number which is a power of two. This induce that the sampling rates are multiples, and the undersampling factors too, which is in disagreement with the condition (15). Within this framework, the sample numbers imposed by the standard Fast Fourier Transform do not satisfy the conditions. It is thus necessary to use an improved version of the FFT algorithm called mixed radix Fast Fourier Transform, making it possible to work with an unspecified number of samples.

In addition, the FFT computation gives the values of the Fourier transform of the sampled signal on the interval $\left[0; \omega_{e\{i\}}\right[$. Because the interval of interest is $\left]-\omega_M; \omega_M\right[$, the result of the FFT has to be duplicate on it, in order to obtain, for each undersampled spectrum, the same block dimension.

Reconstruction algorithm description

As the algorithm is recurrent, an index of iteration l is defined. The computing starts with several versions of the sampled signal at different frequencies $\omega_{e\{i\}}$. For each version, the power spectral density $G^*_{\{i,l=0\}}(\omega)$ is calculated, by Fast Fourier Transform, followed by the duplication on the interval $\left]-\omega_M; \omega_M\right[$.

The next step consists in the multiplication between the several duplicated power spectral densities and in searching the position of the maximum $\omega_{D\max\{l\}}$ in the product. A tiny part ε (a few ten percent) of the identified energy is added to the power spectrum $\hat{G}_{\{l\}}(\omega)$, which has a null initial density and will become the reconstructed PSD:

$$\hat{G}_{\{l+1\}}(\omega) = \hat{G}_{\{l\}}(\omega) + \varepsilon\delta(\omega - \omega_{D\max}) \tag{17}$$

The duplication, due to the sampling, is then applied to this part of energy, which results in a Dirac comb (see equation (11)). The subtraction of this comb to the PSD obtained at the same sampling rate is then computed:

$$G^*_{\{i,l+1\}}(\omega) = G^*_{\{i,l\}}(\omega) - \frac{\varepsilon}{T^2_{e\{i\}}} sha_{\omega_{e\{i\}}}\left(\omega - \omega_{D\max\{l\}}\right) \tag{18}$$

This sequence, described by figure (3), is repeated until obtaining folded up spectra of energy lower than a threshold. One will take, for example, the electronic noise level of which the density, for a given system, is known.

Thus, as the folded up spectra are cut down by the algorithm, the spectrum of the Doppler signal is gradually rebuilt.
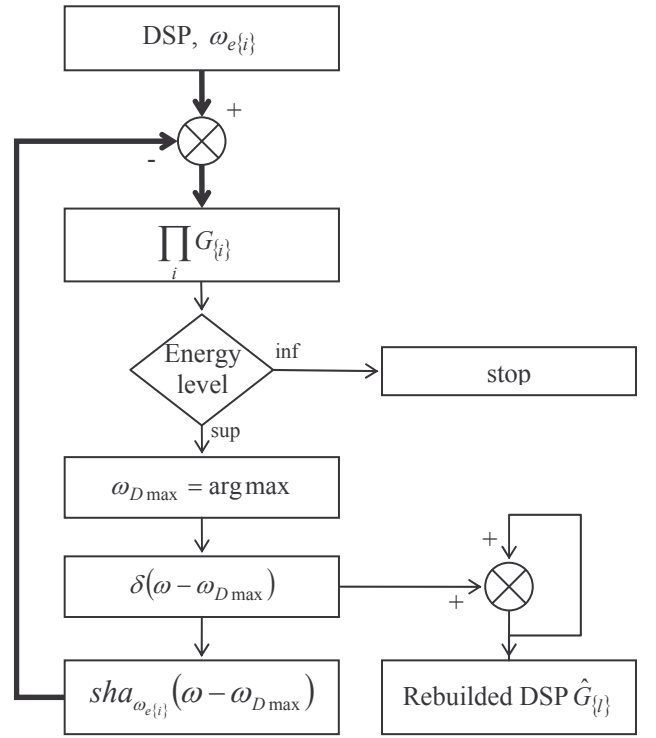

Fig. 3 Synoptic of the reconstruction algorithm. The thick lines represent the parallel processing on each spectral density of index $\{i\}$.

Simulation

In order to validate the functionality of the method, a Doppler signal is simulated on a computer. Various undersampling frequencies are used in order to apply the algorithm and rebuild the power spectral density of the generated signal.

The parameters needed for the signal generation are the central frequency of the spectrum, the bandwidth as well as the signal to noise ratio. The power spectral density is considered to be a Gaussian function of standard deviation taken equal to $\Delta\omega/6$.

The temporal signal is generated starting from the sum of many particle echoes. Each echo consist in a random phase sinusoid with the desired frequency, multiplied by a Gaussian function of standard deviation equal to the inverse of that of the spectrum. Once the individual echoes are summed, the whole energy is calculated in order to define the density of noise according to the desired signal to noise ratio. This noise is then added to the whole particle echoes.

The signal thus generated is used to calculate the reference spectrum (or original spectrum). This same signal is undersampled with various factors $k_{se\{i\}}$ by taking, in the temporal signal, a sample each $k_{se\{i\}}$ in order to obtain the various undersampled signals. The reconstruction algorithm, presented in the preceding section, is then applied to the batch of undersampled signals.

RESULTS AND DISCUSSION

The spectral reconstruction algorithm allows the proper restitution of the original PSD. Figures (4) to (6) presents several examples of spectral rebuilding in different noise and

signal bandwidth situations. Velocity is identical for all curves because the reconstruction only depends on the spectrum's shape, and not on the velocity value.
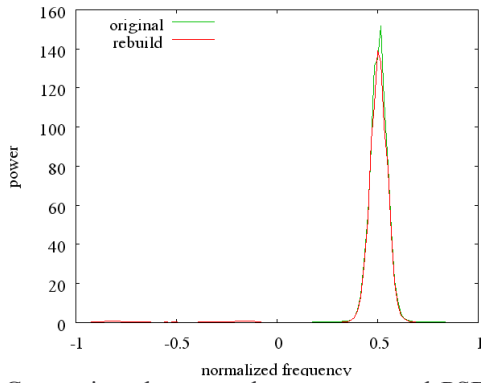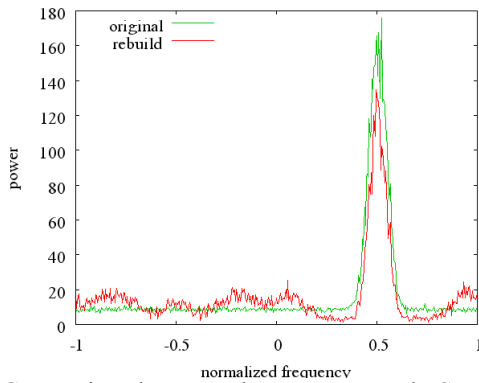

Fig. 4 Comparison between the reconstructed PSD and the one obtained with respect to Shannon theorem for a narrow simulated input spectrum with a signal to noise ration of 100. Frequency is normalized with respect to f_M, and undersampling factors are 2 and 3.

Fig. 5 Comparison between the reconstructed PSD and the one obtained with respect to Shannon theorem for a narrow simulated input spectrum with a signal to noise ratio of 1. Frequency is normalized with respect to f_M, and undersampling factors are 2 and 3.
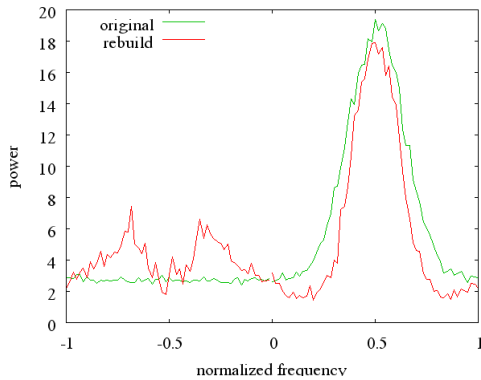

Fig. 6 Comparison between the reconstructed PSD and the PSD obtained with respect to Shannon theorem for a broad simulated input spectrum (condition (11) not respected) with a signal to noise ration of 1. Frequency is normalized with respect to f_M, and undersampling factors are 2 and 3.

Quality level of reconstructed spectrum depends strongly on signal to noise ratio and on spectrum broadness.

In the case of combination of two spectrum dropped down afterwards to 420 samples, the computing duration (*pentium IV* platform at 2.4 GHz with 512 Mo of RAM) is near on 20ms.

This time equals 0.8ms when 48 samples are needed. According to these values, real time processing is possible.

Theory has demonstrated that the boundary factor of this method is the spectrum broadness. Thereby, figure (4) to (6) shows that the quality of the reconstructed PSD depends strongly on signal to noise ratio and on spectrum fitness. Indeed, without respect to this criterion, parts of the spectrum images grow up in different frequency bands where normally no energy exists (presence of parasitic peaks). This phenomenon is generated during spectral products, and come first from white noise, and second from the overlapping of the spectrum copies, issued from the different undersamplings. Additional sampling frequencies can increase the quality of the reconstructed spectrum.

Another way to extract the original PSD is to use the position of the rebuild density as indicator of the position of the original density, and use it for extracting the original PSD from the folded one.

This can be done in observing a window of width ω_{e1}, centered on this position indicator, in the density obtained from the signal undersampled with the factor k_{se1}.

Indeed, although the rebuilt spectrum is denatured beyond the limit given by the condition (13), its position ω_{Dmed} is available until the surrounding of:

$$\Delta\omega < \omega_{e1} \qquad (19)$$

with:

ω_{e1} : highest sampling frequency used.

Moreover, the position of the reconstructed Spectral density is much more consistent than the maximum of the product of the PSD obtained by undersampling. Indeed, unlike the maximum, it is based on the whole spectral information.

Thus, in the case of undersampling factors of 2 and 3, this method would make it possible to pass from a limiting spectrum width of $\omega_M/3$ to ω_M.

CONCLUDING REMARKS

In order to measure velocities beyond the Nyquist limit, a technique based on the use of multiple PRF was proposed. It uses an original algorithm of spectral reconstruction by combination of the information obtained for each sampling rate. Simulations show the applicability of this method in a large variety of situations. However one notes the appearance of a new limit connecting the width of the Doppler spectrum (instead of the maximum frequency) with the exploration depth.

REFERENCES

1. P. Atkinson and J. P. Woodcock, 1982, Doppler ultrasound and its use in clinical measurement, 2nd edition, *Academic Press*.

2. S. Weidong, 1997, An acoustic instantaneous sediment flux profiler for turbulent flow, Phd thesis, *Ecole Polytechnique fédérale de Lausanne*.

3. Sirmans, D. and D. Zrnic and B. Bumgarner, 1976, Extension of Maximum Unambiguous Doppler Velocity by Use of Two Sampling Rates, 17th conference on Radar Meteorology, *Amer. Meteor. Soc.*, Seattle, WA, pp. 23-28.

4. T. Dazhang, S. G. Geotis, R. E. Passarelli Jr., A. L.

Hansen and C. L. Frush, 1984, Evaluation of an Alternating-PRF Method for Extending the Range of Unambiguous Doppler Velocity., 22nd conference on Radar Meteorology, *Amer. Meteor. Soc.*, Zürich, Switzerland, pp.523-527

5. I. Holleman and H. Beekhuis, 2003, Analysis and Correction of Dual-PRF Velocity Data, *Journal of Atmospheric and Oceanic Technology*, 20, pp.443-453.

6. P. Tabary and G. Scialom and U. Germann, 2001, Real-time retrieval of the wind from aliased velocities measured by Doppler radars, *J. Atmos. Oceanic Technol.*, 18, pp. 875-882.

7. S. Liu, H. Wang and Z. Tao, 2003, A simple algorithm for eliminating Doppler velocity aliasing, 31st International Conference on Radar Meteorology, *Amer. Meteor. Soc.*, Seattle, WA

8. C. N. James and R. A. Houze, Jr., 2001, A real-time four-dimensional Doppler dealiasing scheme, *J. Atmos. Oceanic Technol.*, 18, pp. 1674-1683.

9. G. Cloutier, K. K. Shung and L.-G. Durand, 1993, Experimental Evaluation of Intrinsic and Nonstationary Ultrasonic Doppler Spectral Broadening in Steady and Pulsatile Flow Loop Models, *IEEE Transactions on Ultrasonics, Ferroelectrics, and Frequency Control*, 40, pp. 786-795.

ACKNOWLEDGEMENT